The Instability of the Vortex Sheet along the Shear Line①

Gao Shouting (高守亭)

State Key Laboratory of Atmospheric Boundary Layer Physics and Atmospheric Chemistry, Institute of Atmospheric Physics, Chinese Academy of Sciences, Beijing 100029

(Received September 13, 1999, revised March 30, 2000)

ABSTRACT

The traditional Kelvin–Helmholtz notion of studying the shear instability is not suitable for the case associated with shear line with the strong wind shear in the vortex sheet. Since then, the shear instability becomes the instability of the vortex sheet. If the velocity is induced by the vortex sheet, the inequalities $(1 - R_v + Ri_v) > 0$ and $U(y,t) > U(A(t))$ become the criterion of the vortex sheet instability. This criterion indicates that 1) the disposition of environment field restrains the disturbance developing along the shear line. 2) There exist multi-scale interactions in the unstable process of the shear line. The calculation of the necessary condition for the instability is also presented in this paper.

Key words: Shear line, Induced velocity, Instability of the vortex sheet

1. Introduction

The stability problem originally comes from fluid mechanics. About a hundred years ago, Helmholtz (1868), Kelvin (1871) and Rayleigh (1880) revealed that the necessary condition for the unstable shear flow was the existence of a flex point in the basic flow profile, which was further consummated by Fjørtoft (1950) as $U(U - U_s) < 0$ somewhere in the fluid field. Meanwhile, a series of experiments on the instability of pipeline flow (Reynolds, 1883) showed that instability occurs as Reynolds number Re is beyond its critical value ($Re_c \approx 13000$). Kuo (1949) extended Rayleigh's result to rotating atmosphere, and obtained the necessary condition of the atmospheric barotropic instability. Charney (1947) and Eady (1949) proposed the baroclinic instability theory in the 1940's. Howard (1961) developed the Howard's half a circle theorem through studying the stability of the inhomogeneous shear flow. Later on, the studies of stability are extended, from linear, weak nonlinear to nonlinear, from conservative system to dissipative system (Arnol'd, 1965, 1969). Gao and Sun (1986) studied the high order approximation of the symmetric instability by invoking the criterion of Richardson number. Zeng (1986) studied the atmospheric nonlinear instability by generalized variational method. Lu (1989) studied nonlinear barotropic instability with frictional dissipation. Mu (1991) studied nonlinear instability of quasi-geostrophic flow. Besides that, many theses, dissertations and monographes expounded and studied instability problems of different types. Meanwhile, in respect of study methods, normal mode method is mainly used in linear problems, and the high truncated spectrum method, A–B hybrid equation method, variational method and generalized energy method are widely used in nonlinear problems.

①This work was supported by the project on the study of the formative mechanism and predictive theory of the significant climate and weather disaster in China under Grant G 1998040907 and by the key project on the Dynamic Study of Severe Mesoscale Covective Systems sponsored by the National Natural Science Foundation of China under Grant No.49735180.

The several main aspects about stability have been mentioned above, rest of many studies of stability are not listed. So far it is known that the instability about barotropic, baroclinic, linear and nonlinear problems and symmetric instability have been studied meticulously. But the vortex sheet instability along the shear line is rarely studied. Although Scorer (1997), at first, studied the vortex sheet instability in the region with the vertical wind shear and the instability of the steady vortex. The vortex sheet instability with horizontal wind shear is not studied yet. In fact, on the daily weather chart, we can quite often see the shear line with horizontal wind shear on 700 hPa or 850 hPa, so I was motivated to study the vortex sheet instability along the shear line with horizontal wind shear.

2. The instability analysis of vortex sheet along the shear line

Originally, the K–H instability condition of the shear flow was defined as (Scorer, 1997)

$$\frac{(\rho_2-\rho_1)(\rho_2+\rho_1)}{\rho_1\rho_2}\frac{g}{K}<(U_1-U_2)^2 \ , \tag{2.1}$$

where ρ_2, U_2 and ρ_1, U_1 are densities and speeds of basic flow in upper and lower layer respectively. Eq.(2.1) shows that as long as $U_1 \neq U_2$, there is always a range for wave number K. Under the static stable condition and small $\rho_2-\rho_1$, Eq.(2.1) may be written as

$$K> K_c = 2g\frac{\Delta\rho}{\rho}/(\Delta U)^2 \ , \tag{2.2}$$

where $\rho=(\rho_1+\rho_2)/2$, $\rho_2-\rho_1=\Delta\rho$, $\rho_1\rho_2=\rho^2$, and the ratio of K_c/K is the well known Richardson number

$$Ri=\frac{2g\Delta\rho}{K\rho(\Delta U)^2}=\frac{K_c}{K}<1 \ . \tag{2.3}$$

But this perspective did not take two important situations into account, the first is the viscous effect of strong velocity gradient; the second is the effect of a thin vortex sheet due to the increase of the velocity gradient and its discontinuity construction. Since the vorticity in the vortex sheet may produce inductive velocity, the change of stability of the vortex sheet is worthy to be thoroughly studied.

For example, one of the main weather systems producing torrential rain in the Yangtze River valley in China is the unstable vortex sheet along the shear line in lower atmosphere (850–700 hPa). Especially, in Meiyu period, the vortex–street–like mesoscale low–pressure systems often form on the shear line with the inhomogeneous distribution of precipitation. Where there is mesoscale low–pressure system, precipitation intensity is enhanced obviously. According to the multi–scale–system interaction theory, the occurrence of the instability along the shear line must have interactions. From this sense, the study of the vortex sheet instability along the shear line is also the study of multi–scale system interactions.

A sharp velocity gradient constructs a vortex sheet along the shear line due to velocity discontinuity. To describe this situation a coordinate relationship is set up as Fig. 1. In Fig. 1, Δy is the vortex sheet thickness, and the vorticity component is defined as $\eta(=-\partial U(y,t)/\partial y)$.

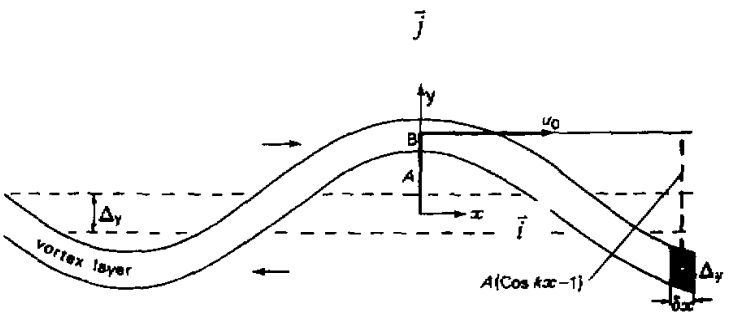

Fig. 1. The schematic vortex sheet along shear line.

If the displacement of disturbance in the vortex sheet is $\zeta = A(t)\cos kx$, the coordinates of wave crest center $B(0, A(t))$ are $[x, A(t)(\cos kx - 1)]$. In the vortex sheet, the vortex element with length δx and width Δy is indicated by $\Delta y \delta x$. According to the inductive velocity theorem of point vortex (Tong et al., 1994), at point B the x component of inductive velocity induced by the vortex element may be written as

$$u_i = \frac{\eta \Delta y \delta x}{2\pi\sqrt{x^2 + (A(t)(\cos kx - 1))^2}} \cdot \frac{A(t)(1-\cos kx)}{\sqrt{x^2 + (A(t)(\cos kx - 1))^2}}$$
$$\approx \frac{\eta \Delta y \delta x}{2\pi x} \cdot \frac{A(t)(1-\cos kx)}{x} . \tag{2.4}$$

For small disturbance, $A(t)$ is also very small, therefore, the terms associated with $A^2(t)$ are neglected here.

From Eq.(2.4), x component of the whole inductive velocity at point B is

$$u_0 = \int_{-\infty}^{\infty} \frac{\eta \Delta y A(t)(1-\cos kx)}{2\pi x^2} dx$$
$$= \frac{\eta \Delta y A(t)}{\pi} \int_{-\infty}^{\infty} \frac{\sin^2 \frac{1}{2} kx}{x^2} dx$$
$$= -\frac{\eta \Delta y A(t)}{\pi} \left[\frac{1}{x} \sin^2 \frac{1}{2} kx \right]_{-\infty}^{\infty} + \frac{\eta \Delta y A(t)}{2\pi} \int_{-\infty}^{\infty} k \frac{\sin kx}{x} dx$$
$$= \frac{\eta \Delta y A(t)}{2\pi} \int_{-\infty}^{\infty} k \frac{\sin kx}{x} dx . \tag{2.5}$$

With $\int_{-\infty}^{\infty} k \frac{\sin kx}{x} dx = k\pi$, Eq.(2.5) may be finally written as

$$u_0(y,t) = \frac{\eta \Delta y A(t) k}{2} . \tag{2.6}$$

Due to the symmetry, the y components of inductive velocity at point B would offset other. As a result, the integrative velocity component in y direction becomes zero.

As long as u_0 is known, at any point x_1 in the vortex sheet, the x component of induc-

tive velocity may be written as

$$u(x_1,y,t)=\int_{-\infty}^{+\infty}\frac{\eta\Delta y A(t)(\cos kx_1-\cos kx)}{2\pi(x-x_1)^2}dx=\frac{1}{2}\eta\Delta y A(t)k\cos kx_1 \ .$$

Replacing x_1 by x, we can get

$$u(x,y,t)=u_0\cos kx=\frac{1}{2}\eta\Delta y A(t)k\cos kx \ . \tag{2.7}$$

As an approximation, Eq.(2.7) is considered to be suitable for the whole vortex sheet with Δy width. Therefore, the inductive velocity components in the vortex sheet may be differentiated with respect to x or y.

Because the inductive velocity is non-divergent, with non-divergent condition $\partial u/\partial x+\partial v/\partial y=0$ and Eq.(2.7), the velocity component v can be obtained:

$$v=-\int(\partial u/\partial x)dy+c(x,t)=-\frac{1}{2}\Delta y A(t)k\cos kx\int\eta dy+c(x,t) \ . \tag{2.8}$$

With $\eta=-\partial U(y,t)/\partial y$ representing the environment vorticity, Eq.(2.8) may be written as

$$v=\frac{1}{2}\Delta y U(y,t)A(t)k\cos kx+c(x,t) \ . \tag{2.9}$$

Since the disturbance is y-axis symmetric, the inductive velocity component v equals zero wherever $x=k\pi\pm\frac{\pi}{2}$, and $2k\pi(k=0,1,2,3\cdots)$. Therefore, $c(x,t)$ in Eq.(2.9) may be determined as

$$c(x,t)=-\frac{1}{2}\Delta y U(A(t))A(t)k\cos kx \ , \tag{2.10}$$

where the condition of $U(A(t))=U(-A(t))$ is also invoked. This condition means that the speeds on both sides of shear line are the same but with opposite sign, so long as they have the same $A(t)$ distance away from the shear line.

So Eq.(2.9) is finally written as

$$v(x,y,t)=\frac{1}{2}\Delta y U(y,t)A(t)k\cos kx-\frac{1}{2}\Delta y U(A(t))A(t)k\cos kx \ . \tag{2.11}$$

From the vorticity equation①

$$\frac{\partial\vec{\omega}}{\partial t}=-(\vec{V}\cdot\nabla)\vec{\omega}-\vec{\omega}\nabla\cdot\vec{V}+(\vec{\omega}\cdot\nabla)\vec{V}+\vec{R}\Lambda(\vec{g}-\vec{a}) \ , \tag{2.12}$$

it is known that for the shear line with quasi-horizontal motion, the vertical vorticity component is the principal component, that is $\vec{\omega}\approx\omega\vec{k}$.

Then we have

$$\begin{aligned}\vec{\omega}(x,y,t)&=\left[\eta+f+\left(\frac{\partial v}{\partial x}-\frac{\partial u}{\partial y}\right)\right]\vec{k}\\&=\left(\eta+f+\frac{1}{2}\Delta y U(A(t))A(t)k^2\sin kx-\frac{1}{2}\Delta y U(y,t)A(t)k^2\sin kx\right.\end{aligned}$$

①see Appendix

$$-\frac{1}{2}\frac{\partial\eta}{\partial y}\Delta y A(t)k\cos kx\Big)\vec{K}\ ,$$

where f is the geostrophic vorticity component, it may be considered as a constant.
In (2.12), $\vec{R},\vec{g}$ and $\vec{a}$ are defined as

$$\vec{R}=\frac{1}{\rho}\nabla\rho=\frac{1}{\rho}\frac{\partial\rho}{\partial y}\vec{J}\ ,$$

$$\vec{g}=-g\vec{k}\ ,\quad \vec{a}=\frac{d\vec{V}}{dt}\approx(\vec{V}\cdot\nabla)\vec{V}=\left[(\bar{u}+u)\frac{\partial}{\partial x}+v\frac{\partial}{\partial y}\right][(\bar{u}+u)\vec{i}+v\vec{j}]\ , \qquad (2.12*)$$

where $\bar{u}(y,t)=\dfrac{U_1(y,t)+U_2(y,t)}{2}$.

With the horizontal non-divergent condition and $\vec{\omega}\approx\omega\vec{k}$, Eq.(2.12) may be written as

$$\frac{\partial\vec{\omega}}{\partial t}=-(\vec{V}\cdot\nabla)\vec{\omega}+\vec{R}\Lambda(\vec{g}-\vec{a})\ . \qquad (2.13)$$

Since $\vec{R}\times\vec{g}=-g\dfrac{1}{\rho}\dfrac{\partial\rho}{\partial y}\vec{i}$ is not along $\vec{k}$, this term has no contribution to the k component of vorticity.

The $\vec{i}$ component in (2.12*) can be rewritten as

$$\left[(\bar{u}+u)\frac{\partial}{\partial x}(\bar{u}+u)+v\frac{\partial}{\partial y}(\bar{u}+u)\right]\vec{i}\approx\left[\bar{u}\frac{\partial u}{\partial x}+v\frac{\partial\bar{u}}{\partial y}\right]\vec{i}$$

$$=[-\bar{u}A(t)\frac{1}{2}\Delta y\eta k^2\sin kx$$

$$+\frac{1}{2}\Delta yU(y,t)\frac{\partial\bar{u}}{\partial y}A(t)k\cos kx$$

$$-\frac{1}{2}\Delta yU(A(t))\frac{\partial\bar{u}}{\partial y}A(t)k\cos kx]\vec{i} \qquad (2.13*)$$

with $A^2(t)$ terms neglected.

Substituting (2.13*) into the second term on the right side of (2.13) we have

$$-\vec{R}\Lambda\vec{a}=R\left(\bar{u}\frac{\partial u}{\partial x}+v\frac{\partial\bar{u}}{\partial y}\right)\vec{K}$$

$$=R\Big[-\frac{1}{2}\bar{u}A(t)\eta\Delta yk^2\sin kx+\frac{1}{2}\Delta yU(y,t)\frac{\partial\bar{u}}{\partial y}A(t)k\cos kx$$

$$-\frac{1}{2}\Delta yU(A(t))\frac{\partial\bar{u}}{\partial y}A(t)k\cos kx\Big]\vec{k}.$$

Because

$$-(\vec{V}\cdot\nabla)\vec{\omega}=-\left[(\bar{u}+u)\frac{\partial}{\partial x}+v\frac{\partial}{\partial y}\right]\left(\eta+f+\frac{1}{2}\Delta yU(A(t))A(t)k^2\sin kx\right.$$
$$\left.-\frac{1}{2}\Delta yU(y,t)A(t)k^2\sin kx-\frac{1}{2}\frac{\partial\eta}{\partial y}\Delta yA(t)k\cos kx\right)\vec{k}$$
$$=[-\frac{1}{2}\bar{u}\Delta yU(A(t))A(t)k^1\cos kx+\frac{1}{2}\bar{u}\Delta yU(y,t)A(t)k^3\cos kx$$
$$-\frac{1}{2}\bar{u}\frac{\partial\eta}{\partial y}\Delta yA(t)k^2\sin kx-\frac{1}{2}\Delta yU(y,t)\frac{\partial\eta}{\partial y}A(t)k\cos kx$$
$$+\frac{1}{2}\Delta yU(A(t))\frac{\partial\eta}{\partial y}A(t)k\cos kx]\vec{k}$$

with $A^2(t)$ terms ignored, Eq.(2.13) may be written as

$$\frac{\partial\vec{\omega}}{\partial t}=-(\vec{V}\cdot\nabla)\vec{\omega}+\vec{R}\Lambda(\vec{g}-\vec{a})$$
$$=[-\frac{1}{2}\bar{u}\Delta yUA(t))A(t)k^3\cos kx+\frac{1}{2}\bar{u}\Delta yU(y,t)A(t)k^3\cos kx$$
$$-\frac{1}{2}\bar{u}\frac{\partial\eta}{\partial y}\Delta yA(t)k^2\sin kx-\frac{1}{2}\Delta yU(y,t)\frac{\partial\eta}{\partial y}A(t)k\cos kx$$
$$+\frac{1}{2}\Delta yU(A(t))\frac{\partial\eta}{\partial y}A(t)k\cos kx]\vec{k}+\vec{R}[-\frac{1}{2}\bar{u}\Delta y\eta A(t)k^2\sin kx$$
$$+\frac{1}{2}\Delta yU(y,t)\frac{\partial\bar{u}}{\partial y}A(t)k\cos kx$$
$$-\frac{1}{2}\Delta yU(A(t))\frac{\partial\bar{u}}{\partial y}A(t)k\cos kx]\vec{k}\,. \tag{2.14}$$

(2.14) indicates that at the points of $\tan kx=0$ and $\cos kx=1$, the condition which satisfies $\partial\vec{\omega}/\partial t>0$ is

$$-\bar{u}U(A(t))k^2+\bar{u}U(y,t)k^2-U(y,t)\frac{\partial\eta}{\partial y}+U(A(t))\frac{\partial\eta}{\partial y}+U(y,t)\frac{\partial\bar{u}}{\partial y}R-U(A(t))\frac{\partial\bar{u}}{\partial y}R>0\,, \tag{2.15}$$

or

$$U(A(t))\left(-\bar{u}k^2+\frac{\partial\eta}{\partial y}-\frac{\partial\bar{u}}{\partial y}R\right)+U(y,t)\left(\bar{u}k^2-\frac{\partial\eta}{\partial y}+\frac{\partial\bar{u}}{\partial y}R\right)>0\,,$$

or

$$-U(A(t))\left(\bar{u}k^2-\frac{\partial\eta}{\partial y}+\frac{\partial\bar{u}}{\partial y}R\right)+U(y,t)\left(\bar{u}k^2-\frac{\partial\eta}{\partial y}+\frac{\partial\bar{u}}{\partial y}R\right)>0\,.$$

$$\text{If}\left(\bar{u}k^2-\frac{\partial\eta}{\partial y}+\frac{\partial\bar{u}}{\partial y}R\right)>0,\ \text{then}-U(A(t))+U(y,t)>0\,,$$

and it leads to

$$U(y,t)>U(A(t))\,.$$

With $\left(\bar{u}k^2-\frac{\partial\eta}{\partial y}+\frac{\partial\bar{u}}{\partial y}R\right)>0$, we have

$$\left(1-\frac{\partial\eta}{\bar{u}k^2\partial y}+\frac{\partial\bar{u}}{\bar{u}k^2\partial y}R\right)>0\,,$$

or

$$(1 - R_i + Ri_d) > 0 \ , \tag{2.17}$$

where R_i is called the shear Richardson number and Ri_d the mixed Richardson number.

If the horizontal gradient of density is not considered, the mixed Richardson number Ri_d equals zero. Therefore, from Eq.(2.17), we get

$$R_i < 1 \ . \tag{2.18}$$

This result is quite similar to the result of the shear instability (Stone, 1966). Eq.(2.16) and Eq.(2.17) together form the necessary condition of the vortex sheet instability along the shear line, that is

$$\begin{cases} (1 - R_i + Ri_d) > 0 \ , \\ \dfrac{U(y,t)}{U(A(t))} > 1 \ , \end{cases} \tag{2.19}$$

where $U(A(t)) \neq 0$.

With $\left(\bar{u}k^2 - \dfrac{\partial \eta}{\partial y} + \dfrac{\partial \bar{u}}{\partial y} R \right) < 0$, we have

$$\begin{cases} (1 - R_i + Ri_d) < 0 \ , \\ \dfrac{U(y,t)}{U(A(t))} < 1 \ . \end{cases} \tag{2.20}$$

Since $\bar{u}k^2 \gg \dfrac{\partial \eta}{\partial y}$ is generally true, and the condition $U(y,t)/U(A(t)) < 1$ in Eq.(2.20) is easily satisfied, the condition $(1 - R_i + Ri_d) < 0$ does not hold. This means that Eq.(2.20) cannot be considered as the criterion of the instability.

The condition given by Eq.(2.19) indicates that there is another option for the disturbance wave length of unstable waves, that is

$$k^2 \geqslant \frac{1}{\bar{u}} \frac{\partial \eta}{\partial y} - \frac{\partial \bar{u}}{\partial y} R \ . \tag{2.21}$$

For the shear line with the vortex sheet in the Yangtze River valley, $\partial \eta / \partial y$ must be very large, generally in the order of magnitude of 10^{-7}–10^{-8} (if $\partial \eta / \partial y$ is relatively small, the shear line is not considered as the shear line with the vortex sheet). Therefore, in inequality (2.21), the term $\dfrac{1}{\bar{u}} \dfrac{\partial \eta}{\partial y} \sim 10^{-8} \sim 10^{-9}$ is a principal term compared with $-\dfrac{\partial \bar{u}}{\partial y} R \sim 10^{-11} \sim 10^{-12}$. The wave length $L = \dfrac{1}{k}$, for the optimum disturbance determined by the term ordinarily ranges from 10 km to 100 km approximately. This is the typical scale for meso–small–scale disturbance along the shear line. From the above theoretical analysis, it is known that if the vortex sheet is very strong, and $\partial \eta / \partial y$ is very large (for example, $\partial \eta / \partial y \sim 10^{-5} \sim 10^{-6}$), the wave length $L = \dfrac{1}{k}$ of the optimum disturbance will be 600 m to 1000 m, and this scale is corresponding to the scale of the rain mass. It is clear that the sharper the shear line is, the shorter the unstable disturbance wave length.

3. A case study of the vortex sheet instability along the shear line

From 21 to 24 July, 1998, the vortex sheet instability occurs along the shear line over the Yangtze River valley. At 00UTC 21 July, there is a west–east oriented shear line at 700 hPa near 30°N over the Yangtze River valley (Fig. 2). Corresponding to this shear line, there is a rainfall zone from 110°E to 118°E in the Yangtze River valley with daily averaged rainfall amount of about 15 mm.

24 hours later, at 00UTC 22 July (Fig. 3), the rainfall amount related to the shear line is more than that on 21 July, and the rainfall distribution is inhomogeneous. In the middle part of the shear line, near 110°E, there is the largest rainfall center with daily rainfall of more than 100 mm (Fig. 4), it hints the development of a mesoscale system along the shear line with the effect of instability.

Figures 5 and 6 show the streamline distributions at 00UTC 23 July and at 00UTC 24 July respectively. From these two figures, it can be clearly seen that with the mesoscale system developing (because the mesoscale system is hardly depicted in the streamline map), the shear line is disturbed and transforms into a wave–like pattern. Corresponding to this shear line, the distribution of the daily rainfall shows several torrential rain centers (Fig. 7) e.g. the center

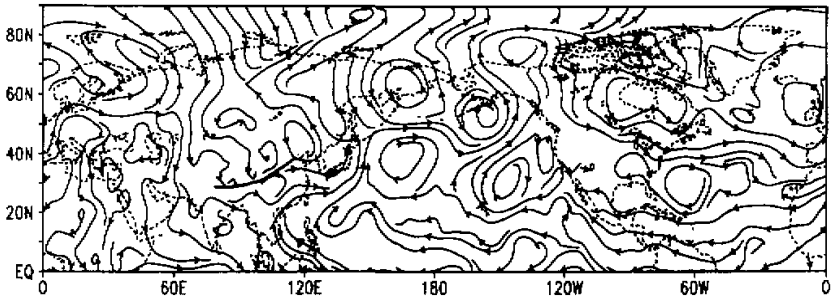

Fig. 2. The streamline distribution at 700 hPa, at 00UTC 21 July 1998.(The bold and full line indicates the shear line).

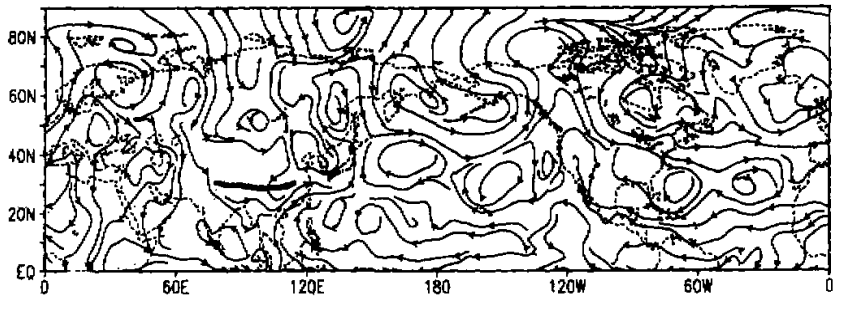

Fig. 3. The streamline distribution at 700 hPa, at 00UTC 22 July 1998. (The bold and full line indicates the shear line).

near 30°N, 118°E with 80 mm rainfall or more, the center near 28°N, 110°E with 60 mm or more, the center near 30°N, 114°E with 50 mm or more. These are an indication of activities of mesoscale rain mass induced by the instability along the shear line.

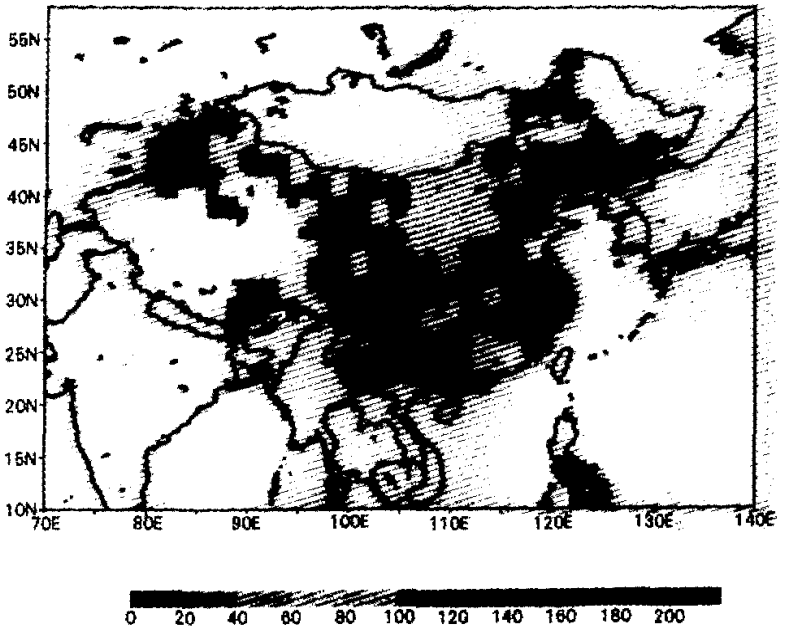

Fig. 4. The precipitation distribution at 00UTC 22 July 1998.

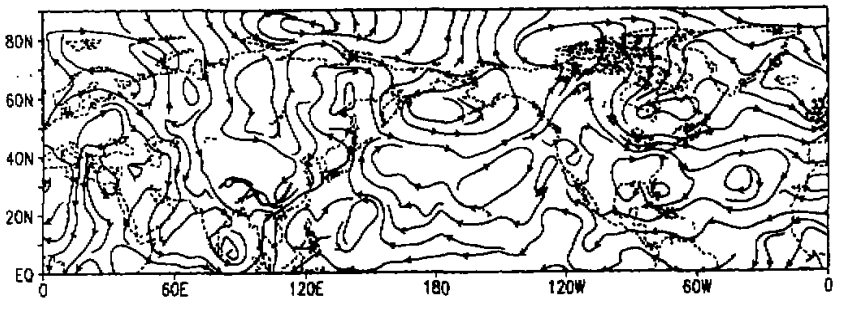

Fig. 5. The streamline distribution at 700 hPa, at 00UTC 23 July 1998, (The bold and full line indicates the shear line).

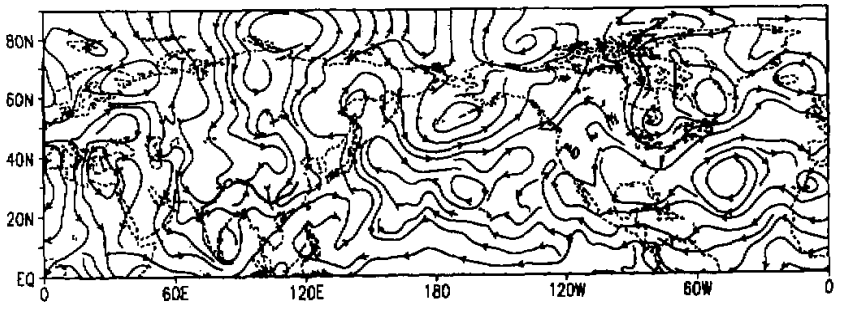

Fig. 6. The streamline distribution at 700 hPa, at 00UTC 24 July 1998.(The bold and full line indicates the shear line).

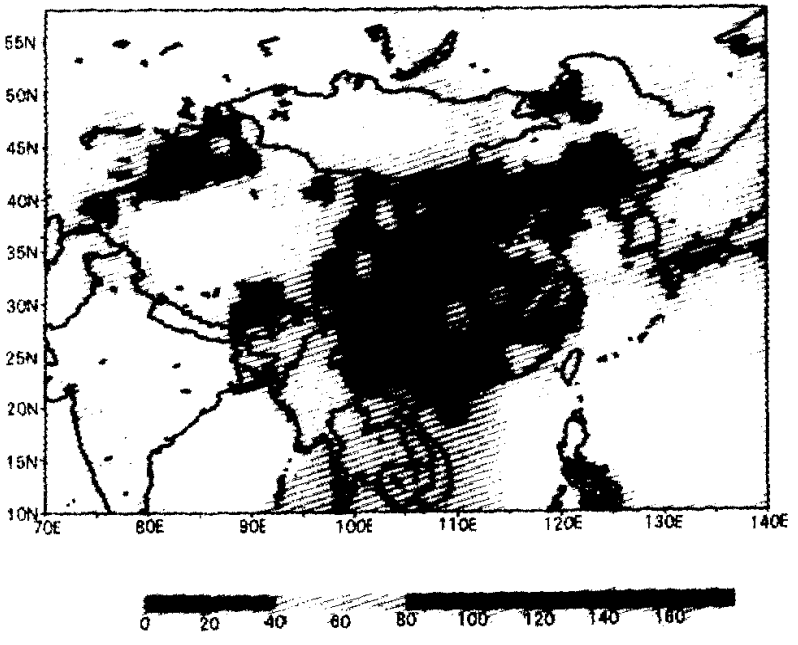

Fig. 7. The precipitation distribution at 00UTC 23 July 1998.

Fig. 8 shows the wind vector distribution at 700 hPa, at 00UTC 23 July. From Fig. 8, it can be seen that there exists evident wind convergence along the shear line. In the west part of the shear line, the wind vector converges and meets with joining point, it means that at the joining point, the mesoscale system must occur.

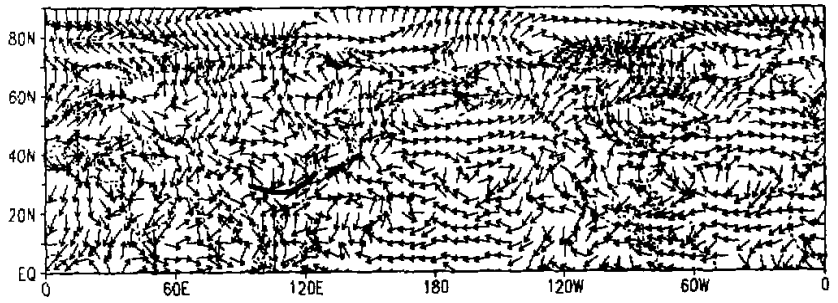

Fig. 8. The horizontal wind vector distribution at 700 hPa, at 00UTC 23 July 1998.

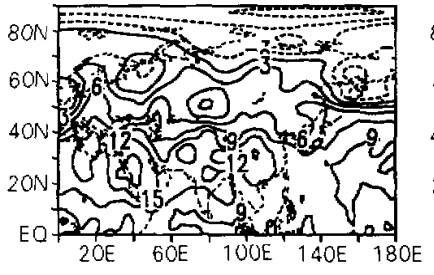

Fig. 9. The temperature distribution at 700 hPa, at 00UTC 22 July 1998.

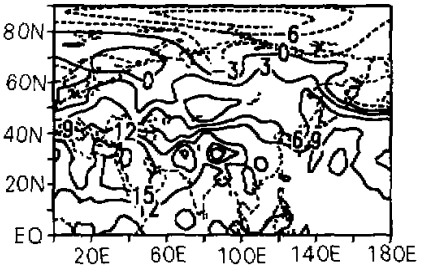

Fig. 10. The temperature distribution at 700 hPa, at 00UTC 23 July 1998

Figures 9 and 10 show the temperature distribution at 700 hPa at 00UTC 22 July, and at 00UTC 23 July at 700 hPa, respectively. The sharp temperature gradient appears near 40°N, but near 30°N, the temperature gradient is relatively weak. At 00UTC 23 July, at 700 hPa the temperature distribution shows that near 30°N the temperature gradient gets larger than that at 00UTC 22 July. It implies that from 00UTC 22 to 00UTC 23 July baroclinity becomes stronger due to the convergence of cold / warm air from north / south side of the shear line. This also leads to the vortex sheet instability along the shear line.

According to the necessary condition of the vortex sheet instability mentioned in last section, several parameters are calculated and compared with their theoretical values. The result shows that after at 00UTC 22 July, the necessary condition is satisfied for the vortex sheet instability. So the development of mososcale system on the shear line is inevitable. For $P=700$ hPa and $R=$constant, the absolute temperature T may be obtained from the temperature distribution on 700 hPa. So it is very easy to get the density value according to $\rho=\frac{P}{RT}$. At 00UTC 23 July near 30°N, 110°E, for example, it is found that near the center of the shear line $\bar{u}=3.5$ m s^{-1}, $\partial\eta/\partial y=3.5\times10^{-7}$ m^{-1}s^{-1}, $\partial\bar{u}/\partial y=-0.2\times10^{-3}$ s^{-1}, $R=\frac{1}{\rho}\partial\rho/\partial y=-\frac{1}{T}\partial T/\partial y=0.8\times10^{-7}$ m^{-1}. As a result, the disturbance wave length is $L\approx 3.5$ km. Near

the center, there exists the indication of vortex sheet instability $U(y,t) > U(A(t))$ according to Eq.(2.19).

4. Summary

The necessary condition of the vortex sheet instability is obtained from manipulating vorticity equation. However, the final expression of this theory only aims at specific points along the shear line. A brief case study shows that the instability does occur at some specific points along the shear line, which implies that the shear line is unstable. As for the application, however, synoptic knowledge and forecast experience are often required in order to find those specific points and the position of disturbance wave crest and trough.

In this study, the normal method is avoided, because in the normal mode, method ϖ in the normal mode version must be expressed as wave form, while the vorticity distribution has no wave-like form. So here we adopted the local or total change of the vorticity to explore the occurrence mechanism of the instability. Finally it must be pointed out that the vortex sheet instability along the shear line is only a form of the shear line instability and the other forms of the instability of the shear line are not discussed in this paper, such as the instability induced by the gravity wave chase and so no.

Appendix

$$\frac{d\vec{\varpi}}{dt} = \vec{\varpi} \cdot \nabla \vec{v} - \vec{\varpi} \cdot \nabla \cdot \vec{v} + \frac{\nabla \rho \times \nabla p}{\rho^2} \quad . \tag{1}$$

In Eq.(1), $1/\rho \nabla p$ is displaced by the momentum equation, that is

$$\frac{1}{\rho} \nabla p = \vec{g} - \frac{d\vec{v}}{dt} - f\vec{k} \times \vec{v} \quad . \tag{2}$$

Substituting (2) into (1), we have

$$\frac{d\vec{\varpi}}{dt} = \vec{\varpi} \cdot \nabla \vec{v} - \vec{\varpi} \cdot \nabla \cdot \vec{v} + \frac{1}{\rho} \nabla \rho \times \left(\vec{g} - \frac{d\vec{v}}{dt} - f\vec{k} \times \vec{v} \right) \quad . \tag{3}$$

Since in the vicinity of the shear line the wind almost blows along the shear line, $f(\vec{u} + u)\vec{j}$ is the dominant component of Coriolis force. Besides the density gradient can be expressed by $\vec{R} = \frac{1}{\rho} \nabla \rho = \frac{1}{\rho} \frac{\partial \rho}{\partial y} \vec{j}$, which means $\vec{R} \times f(\vec{u} + u)\vec{j} = 0$. For this reason, Eq.(3) may be written as

$$\frac{d\vec{\varpi}}{dt} = \vec{\varpi} \cdot \nabla \vec{v} - \vec{\varpi} \cdot \nabla \cdot \vec{v} + \frac{1}{\rho} \nabla \rho \times (\vec{g} - \vec{a}) \quad , \tag{4}$$

where $\vec{a} = \frac{d\vec{v}}{dt}$.

REFERENCES

———V. I., 1965: Condition for nonlinear stability of stationary plane curvilinear flows of an ideal fluid. *Dokl. Akad. Nauk. SSSR*, **165**, 975–978 (English Transl: Soviet Math., 6, 773–777).

Arnol'd, V. I., 1969: On a priori estimate in the theory of hydrodynamic stability. *Amer. Math. Soc. Transl.*, **19**, 267–269.

Charney, J. G., 1947: The dynamics of long waves in a baroclinic westerly current. *J. Meteor.*, **4**, 135–163.

Eady, E. T., 1949: Long waves and cyclone waves. *Tellus*, **1**, 33–52.

Fjørtoft, R., 1950: Application of integral theorems in deriving criteria of stability for laminar flows and for baroclinic circular vortex. *Geophys. Publ.*, **17(b)**, 1–52.

Gao Shouting, and Sun Shuqing, 1986: The instability of mesoscale fluctuation distinguished with Richardson number. *Chinese J. Atmos. Sci.*, **10**, 171–182.

Helmholtz, H., 1868: On discontinuous movements of fluids. *Phil. Mag.* **(4)36**, 337–346.

Howard, L. N., 1961: Note on a paper of John W. Miles. *J. Fluid Mech.*, **10**, 509–512.

Kelvin, W., 1871: The influence of wind on waves in water supposed frictionless. *Phil. Mag.*, **(4)42**, 368–374.

Kuo, H. L., 1949: Dynamic instability of two-dimensional non-divergent flow in a barotropic atmosphere. *J. Meteor.*, **6**, 105–122.

Lin, C. C., 1955: *The Theory of Hydrodynamic Stability*. Cambridge University Press, 155 pp.

Lu Weisong, 1989: The nonlinear stability of shear flow in the atmosphere with friction and dissipation. *Acta Meteorologica Sinica* **47**, 412–423 (in Chinese).

Mu, M., 1991: Nonlinear stability criteria for motions of multi-layer quasi-geostrophic flow. *Science in China*, B, **34**, 1516–1528.

Rayleigh, Lord, 1880: On the stability, or instability, of certain fluid motions. *Proc. Lon. Math. Soc.*, **11**, 57–70.

Reynolds, O., 1883: An experimental investigation of the circumstances which determine whether the motion of water shall be direct or sinuous, and of the law of resistance in parallel channels. *Phil. Trans. Roy. Soc.*, **174**, 935–982.

Richard S. Scorer, 1997: *Dynamics of Meteorology and Climate*, PRAXIS Publishing LTD, 686 pp.

Scorer, R. S, 1997: *Dynamics of Meteorology and Climate*, PRAXIS publishing, LTD, 74–79.

Stone, P. H., 1966: On non-geotrophic baroclinic stability. *J. Atmos. Sci.*, **23**, 390–400.

Stone, P. H., 1966: On non-geostrophic barochnic stability. *J. Atmos. Sci.*, **23**, 390–400.

———, 1992: *Dynamic Stability Theorem*, China Meteorological Press, 298 pp.

Tong Binggang, Yin Xieyuan, and Zhu Keqin, 1994: *The Vortex Motion Theory*, Chinese University of Science and Technology Press, 76–79.

Zeng Q. C., 1986: Non-geostrophic instability. *Science in China*, Series B, 29, 535–542.